

Nucleon-Nucleon Scattering with Perturbative Pions: The Uncoupled P -Wave Channels

J. B. Habashi*

Department of Physics, University of Arizona, Tucson, AZ 85721, USA

We study the uncoupled P -wave channels of nucleon-nucleon scattering in an effective field theory (EFT) including a perturbative dibaryon field and perturbative pions. Good agreement between EFT results and the Nijmegen partial wave analysis is observed up to a center-of-mass momentum $k \sim 400$ MeV. Using a new method that combining renormalization and fitting together, the long-standing convergence problem of EFTs in these channels with perturbative pions, for momenta above the pion mass is addressed from a new perspective.

I. INTRODUCTION

Half a decade after Weinberg's seminal work [1, 2] on effective field theories (EFTs) of nuclear physics with non-perturbative pions [3, 4], Kaplan, Savage and Wise (KSW) introduced an EFT with a new power counting (PC) that treats pion interactions perturbatively [5–7]. For a recent review of different PC and progress in nuclear EFTs see [8, 9]. Similar to Weinberg's PC, i.e. naive dimensional analysis (NDA) [10, 11], the KSW PC requires resummation of the contact C_0 interaction at leading order (LO) for the S -wave channels. This reproduces the bound/virtual state poles seen in nature. Pions, however, were included perturbatively starting at next-to-leading order (NLO) as justified by empirical evidence from the spin-singlet S -wave channel which suggests that the chiral expansion parameter for nucleon-nucleon (NN) scattering is roughly $1/3$. This agrees with the theoretical expansion in Q/Λ_{NN} where $Q \sim 100$ MeV is a typical low energy scale and $\Lambda_{NN} = 16\pi f_\pi^2 / (m_N g_A^2) \approx 300$ MeV, with $g_A = 1.25$ and the pion decay constant $f_\pi \simeq 92$ MeV.

In the S -wave channels, pions at NLO only account for half of the effective range r_0 , so C_2 is promoted to NLO in the KSW PC, even though it appears at a higher order in NDA. By using the same argument as in Ref. [10], one can show that changing the PC for C_2 affects higher order low energy constants (LECs) in the S -wave channels as well. In the other channels¹, the LECs of four-nucleon contact interactions in the KSW PC have an extra power of M_{lo}/M_{hi} relative to NDA. For example, in the P -wave channels the LO phase shift is zero, and at NLO and next-to-next-to-leading order (NNLO) there are only contributions from the one-pion exchange (OPE) potential; C_2 in these channels appears at next-to-next-to-next-to-leading order (N³LO) [7, 12].

In the 1S_0 channel the KSW PC converges for momenta up to $M_{hi} \sim \Lambda_{NN} \sim 300$ MeV, however Fleming *et al.* [12, 13] show that in the lower spin-triplet channels the PC does not converge at NNLO. Additionally, Kaplan and Steele [14] argue that the slow convergence problem of the KSW PC above the pion mass is due to higher energy physics and is not related to pion interactions which mostly affect lower energies.

One way of incorporating correlated high energy physics is by introducing a dibaryon field. They were first introduced in the context of nuclear EFTs by Kaplan [15], and have since been studied in the S -wave channels of NN scattering [16–21]. These studies were carried out in various energy regimes, both with perturbative and non-perturbative pions². Comparing the pionless and pionful results of Ref. [20] for momenta up to $k \sim 400$ MeV strongly suggests that pions can be treated perturbatively in the presence of dibaryon fields. This begs the question: can pion

* jbalalhabashi@email.arizona.edu

¹ Except for the contact interactions of the mixing channel $^3S_1 - ^3D_1$, like $C_2^{(SD)}$, that appear at the same order as NDA.

² For applying a dibaryon as a resonance field in all partial waves of a pionless EFT see [22].

interactions in other channels be treated perturbatively in the presence of an auxiliary field? Although it might be new in nuclear EFTs, a similar idea was pursued in the context of quantum interactions. In earlier papers [23, 24], Weinberg showed that quantum interactions can be treated perturbatively by introducing a heavy quasi-particle state.

In addition to the work on S -wave channels of NN scattering that suggest that pions can be treated perturbatively with a dibaryon field, there is phenomenological motivation, especially for the uncoupled P -wave channels, for including a dibaryon field. That is the phase shift in these channels decreases almost linearly at larger momenta, i.e. $\delta \propto -k$, however promoting the contact C_2 interaction to NLO gives $\delta \propto k^3$ [25]. But with a dibaryon field one can get a tune-able linear function (see section IV for further discussion on this subject).

By adding a dibaryon field we include an infinite subset of correlated contact interactions and thus incorporate higher energy physics. We hope that one result of this is to push the breakdown scale of the theory to ~ 1 GeV rather than ~ 300 MeV. We also hope that pion interactions become perturbative by including a dibaryon field. As a result the PC will differ from NDA.

In our PC chiral-symmetry-breaking (CSB) contact interactions appear at higher orders after chiral ones. By looking at diagrams and keeping track of divergent terms proportional to m_π^{2m} we can get an estimate of the PC [6, 7]. After factoring out $4\pi/m_N$, the PC of contact interaction LECs for $n \geq 0$ and $m \geq 1$ is

$$C_{2n} \sim \mathcal{O}\left(\frac{1}{M_{lo}M_{hi}^{2n}}\right), \quad (1)$$

$$D_{2n+2m} m_\pi^{2m} \sim \mathcal{O}\left(\frac{M_{lo}^{2m-2}}{M_{hi}^{2n+2m-1}}\right) \sim \left(\frac{M_{lo}}{M_{hi}}\right)^{2m-1} \mathcal{O}\left(\frac{1}{M_{lo}M_{hi}^{2n}}\right). \quad (2)$$

For a specific n , C_{2n} appears at N^{2n} LO. The CSB LECs with the same powers of momentum as C_{2n} s start to appear at one order higher. We know that m_π^2 appears whenever there is chiral symmetry breaking, hence counting divergent terms proportional to m_π^{2m} suggests that symmetry breaking is down by appropriate powers of M_{lo}/M_{hi} each time. For example the PC of $D_{2n+2m} m_\pi^{2m}$ suggests that adding m_π^{2m} is equivalent to adding $2m - 1$ powers of M_{lo}/M_{hi} to the normal PC of the same order LECs, i.e. C_{2n} s. This observation is useful for determining the PC of CSB LECs of dibaryon fields after finding the PC for their chiral counterparts.

Similar to the PC of NDA and KSW, a cancellation between C_0 and the analytic part of loop integrals results in a resummation of diagrams. The resummation only happens in the S -wave channels, and all other LECs are perturbative, e.g. a C_2 appears at NNLO in all channels. The first CSB contact interaction D_2 appears at NLO in the S -wave channels, and in all channels D_4 appears at N^3 LO.

As demonstrated in this paper, the dibaryon field is perturbative and appears at NLO. For the uncoupled P -wave channels the PC of the LECs associated with the dibaryon field is

$$g_1 \sim \mathcal{O}\left(\frac{1}{M_{hi}}\right), \quad h_{1+2m} m_\pi^{2m} \sim \mathcal{O}\left(\frac{M_{lo}^{2m-1}}{M_{hi}^{2m}}\right), \quad (3)$$

$$\Delta \sim \mathcal{O}\left(\frac{M_{lo}^2}{M_{hi}}\right), \quad \omega_{2m} m_\pi^{2m} \sim \mathcal{O}\left(\frac{M_{lo}^{2m+1}}{M_{hi}^{2m}}\right), \quad (4)$$

where g_1 and Δ are chirally symmetric dibaryon LECs with naive or simple PC, and $h_{1+2m} m_\pi^{2m}$ and $\omega_{2m} m_\pi^{2m}$ are CSB dibaryon LECs with the same type of interaction as g_1 and Δ , respectively. In principle we should be able to derive this PC for each partial wave by using a non-relativistic version of the method in Ref. [10], but such a calculation is beyond the scope of this paper. We find that the PC in Eqs. (3)-(4) works at least up to NNLO for the uncoupled P -wave channels. The observation about the relation between m_π^{2m} and $M_{lo}^{2m-1}/M_{hi}^{2m-1}$ for $D_{2n+2m} m_\pi^{2m}$ is key in deducing the CSB PC in Eqs. (3)-(4). As we see, the first CSB LECs for P waves appear at NNLO.

The rest of the paper is organized as follows. In Sec. II, the Lagrangian and PC are discussed in more detail. The T matrix and a new method of renormalization and parameter fitting are explained in Sec. III. In the same section, the NLO and NNLO regulator-independent T matrices are calculated. In Sec. IV, we fit the EFT phase shifts to the

Nijmegen partial wave analysis (PWA) [26, 27]. We conclude in Sec. V. App. A gives details of the off-shell NLO T matrices, analytic expressions for pion-dibaryon loop integrals and the regulator dependence of LECs. In App. B, a second method of renormalization and parameter fitting is presented and discussed.

II. LAGRANGIAN AND POWER COUNTING

We consider an NN scattering system for which the Lagrangian is invariant under Lorentz transformations (in the form of reparameterization invariance [28, 29]), parity and time-reversal transformations, and conserves baryon number. Similar to NDA [10, 11], the low and high energy scales are taken to be $M_{l_0} \sim 300$ MeV and $M_{h_i} \sim 1$ GeV, and pions are needed as explicit degrees of freedom because their mass $m_\pi \simeq 140$ MeV is of order M_{l_0} . Spontaneous breaking of chiral $SU(2)_L \times SU(2)_R$ symmetry of QCD into the $SU(2)_V$ subgroup of isospin [1, 2, 30] is our guide for the form of interactions in the EFT, with an isospin-triplet of pions π_a ($a = 1, 2, 3$). Chiral-symmetric interactions are included via the chiral covariant derivatives of pion and nucleon fields, however CSB interactions proportional to quark masses or m_π^2 are constructed using the components of $SO(4)$ vectors. Finally, in order to include physics of energies above the pion mass, we introduce an auxiliary odd-parity dibaryon field $\phi_{i,a}^{(s)}$ [15] for each channel with a sign parameter $\eta^{(s)}$. The most general Lagrangian is³

$$\begin{aligned} \mathcal{L} = & N^\dagger \left[i\partial_0 + \frac{\vec{\nabla}^2}{2m_N} - \frac{g_A}{2f_\pi} \tau_a \left(\vec{\sigma} \cdot \vec{\nabla} \pi_a \right) \right] N + \frac{1}{2} \pi_a \left(\partial_0^2 - \vec{\nabla}^2 + m_\pi^2 \right) \pi_a \\ & + \eta^{(s)} \phi_{i,a}^{(s)\dagger} \left[i\partial_0 + \frac{\vec{\nabla}^2}{4m_N} - \left(\Delta^{(s)} + \omega_2^{(s)} m_\pi^2 \right) \right] \phi_{i,a}^{(s)} + \sqrt{\frac{4\pi}{m_N}} \left(g_1^{(s)} + h_3^{(s)} m_\pi^2 \right) \left(\phi_{i,a}^{(s)\dagger} N^T P_{i,a}^{(s)} N + \text{H.c.} \right) \\ & - \frac{4\pi}{m_N} C_2^{(s)} \left(N^T P_{i,a}^{(s)} N \right)^\dagger \left(N^T P_{i,a}^{(s)} N \right) + \dots, \end{aligned} \quad (5)$$

where $s = {}^1P_1, {}^3P_0, {}^3P_1$, and the sum over the vector index i and isospin index a are implicit. LECs are also labeled for each channel separately. In the above Lagrangian, $\vec{\sigma}$ (τ_a) are the Pauli matrices in spin (isospin) space,

$$P_i^{({}^1P_1)} = \frac{\sqrt{3}}{2\sqrt{2}} \left(\frac{-i\overleftrightarrow{\nabla}_i}{2} \right) (i\sigma_2) (i\tau_2), \quad (6)$$

$$P_a^{({}^3P_0)} = \frac{1}{2\sqrt{2}} \left(\frac{-i\overleftrightarrow{\nabla}_i}{2} \right) (i\sigma_2 \sigma_i) (i\tau_2 \tau_a), \quad (7)$$

$$P_{i,a}^{({}^3P_1)} = \frac{\sqrt{3}}{4} \epsilon_{ijk} \left(\frac{-i\overleftrightarrow{\nabla}_j}{2} \right) (i\sigma_2 \sigma_k) (i\tau_2 \tau_a) \quad (8)$$

are the projection operators on respectively the 1P_1 , 3P_0 and 3P_1 channels [12, 13], with $\overleftrightarrow{\nabla} \equiv \overrightarrow{\nabla} - \overleftarrow{\nabla}$. The “...” indicates higher order terms with more fields, derivatives and powers of m_π^2 . For a nucleon-dibaryon interaction with ℓ derivatives that appears at NLO we need at least $\ell + 1$ dibaryon LECs to renormalize the loop integrals at higher orders. For the P waves with $\ell = 1$, we need two LECs which are present as Δ and g , and there is no need for higher derivative dibaryon interactions, as their effects are accounted for by higher-order contact terms.

In contrast to the usual notation in most of the literature, $4\pi/m_N$ has been factored out of the LECs, and the convention for definitions of the T matrix and potential throughout the paper is

$$\overline{T} \equiv \frac{m_N T}{4\pi}, \quad \overline{V} \equiv \frac{m_N V}{4\pi}. \quad (9)$$

³ We assume that only nucleon fields interact with pions and not the dibaryon field. For a dibaryon field interacting with pions see [17–19].

A typical LEC \mathbf{g} and consequently observables like the T matrix and phase shift are expanded at each order of the perturbation

$$\mathbf{g} = \mathbf{g}^{(0)} + \mathbf{g}^{(1)} + \mathbf{g}^{(2)} + \dots, \quad (10)$$

$$\bar{T} = \bar{T}^{(0)} + \bar{T}^{(1)} + \bar{T}^{(2)} + \dots, \quad (11)$$

$$\delta = \delta^{(0)} + \delta^{(1)} + \delta^{(2)} + \dots, \quad (12)$$

where the superscripts $n = 0, 1, 2, \dots$ indicate LO, NLO, NNLO and so on. Each channel has its own LECs, but the channel superscripts s will be dropped throughout this paper for simplicity. According to the PC, the LECs appearing at each order are:

$$\begin{aligned} \text{LO} &: \text{---} \\ \text{NLO} &: \Delta^{(0)}, g_1^{(1)}, \bar{\pi} \\ \text{NNLO} &: \Delta^{(1)}, \omega_2^{(1)} m_\pi^2, g_1^{(2)}, h_3^{(2)} m_\pi^2, C_2^{(2)}, \bar{\pi} \bar{\pi} \end{aligned} \quad (13)$$

where $\bar{\pi} \bar{\pi}$ means iteration of the OPE potential. Radiation and soft pion interactions are not considered in the up-to-NNLO calculations of this paper. Thus similar to Ref. [12] for the P waves we include only iterations of the OPE potential. These iterations contain infrared enhancements [1, 2] relative to multiple-pion-exchange potentials with the same number of pion fields [31]. Note that the residual mass of the dibaryon always comes with a factor of the nucleon mass m_N , therefore $\Delta^{(0)}$ is a LO LEC with the same size as the kinetic term, but the smallness of the nucleon-dibaryon coupling g_1 means that it first appears at NLO.

There is no difference in the Feynman rules of chiral and CSB LECs with the same number of derivatives or momenta that appear at the same order in the perturbation. Thus we define

$$\tilde{\Delta}^{(1)} \equiv \Delta^{(1)} + \omega_2^{(1)} m_\pi^2 \quad (14)$$

$$\tilde{g}_1^{(2)} \equiv g_1^{(2)} + h_3^{(2)} m_\pi^2, \quad (15)$$

which are used in the NNLO calculations. Whenever a new LEC appears at a given order of perturbation theory, e.g. $\omega_2^{(1)}$ and $h_3^{(2)}$, an additional fitting parameter is needed as well. The NLO LECs and NNLO C_2 do not run with the regulator, and we give an estimate of their size in terms of M_{lo} and M_{hi} in Sec. IV.

In this paper, we renormalize in two different ways. In the next section, we maximally exploit the non-locality of the dibaryon field by absorbing a part of the nonanalytic effects of pion interactions in its NNLO LECs. In the second method detailed in App. B, nonanalytic pion effects get absorbed in a redefinition of dibaryon NLO LECs by re-fitting them at NNLO. Although this may work in special cases and at lower orders of the perturbation, we see that nonanalytic effects of pion interactions, both chiral and CSB parts, can have large effects on LECs at higher orders of the perturbation, as has been observed in [12, 13].

III. T MATRIX AND RENORMALIZATION

The T matrix of non-relativistic quantum systems has been studied extensively, for example see [32]. We are specifically interested in the T matrix that is directly related to the scattering amplitude via Feynman diagrams in an EFT⁴. Therefore for a non-relativistic EFT we use the Lippmann-Schwinger equation (LSE) for a systematic

⁴ Note that for the scattering amplitude \mathcal{A} we have $\mathcal{A} = -\bar{T}$.

expansion of T in a perturbative scheme. The off-shell LSE for the T matrix in the momentum space is

$$T(\vec{p}', \vec{p}, k) = V(\vec{p}', \vec{p}) + \int \frac{d^3 q}{(2\pi)^3} V(\vec{p}', \vec{q}) G(\vec{q}, k) T(\vec{q}, \vec{p}), \quad (16)$$

where $k = \sqrt{m_N E}$ and

$$G(\vec{q}, k) = \frac{m_N}{k^2 - q^2 + i\epsilon}. \quad (17)$$

is the non-relativistic Schrödinger propagator. The potential $V(\vec{p}', \vec{p})$ is given by tree level diagrams in the EFT. The total spin s and the total angular momentum j are conserved, and if we label the angular momentum between incoming and outgoing particles by ℓ and ℓ' respectively, the projected off-shell T matrix with the convention in Eq. (9) is

$$\bar{T}_{\ell, \ell'}(p', p) = \bar{V}_{\ell, \ell'}(p', p) + \frac{2}{\pi} \sum_{\ell''} \int^{\Lambda} dq q^2 \frac{\bar{V}_{\ell, \ell''}(p', q) \bar{T}_{\ell'', \ell'}(q, p)}{k^2 - q^2 + i\epsilon}, \quad (18)$$

where the angular momenta ℓ , ℓ' and ℓ'' run over $j - s$ to $j + s$. For the uncoupled channels $\ell = \ell' = \ell''$ and we ignore the summation. In the above equation, the sharp-cutoff regulator is only for the magnitude of 3-momentum, and there is no breaking of rotational invariance.

For the sharp cutoff with $\Lambda \rightarrow \infty$ limit, Phillips *et al.* [33] show that results of loop integration are equivalent to the PDS (power divergence subtraction) scheme of Ref. [6, 7] if poles in dimensions other than $D = 4$ are subtracted. In the sharp-cutoff scheme of this paper, we keep only the divergent and finite terms in loop diagrams. Although terms that vanish as $\Lambda \rightarrow \infty$ give insight into the size of the theoretical error and the next order LECs, they are omitted because they are not important for the purpose of renormalization.

To calculate the T matrix at each order in the perturbation, we calculate the tree level off-shell T matrix or potential, and then replace the T matrix in the integrand of Eq. (18) with the potential to get the T matrix of next order and so on. The phase shift and T matrix are related to each other through the unitarity condition of the S matrix

$$S = e^{2i\delta} = 1 - 2ik\bar{T}. \quad (19)$$

For the P -wave channels, the LO phase shift $\delta^{(0)} = 0$ because the T matrix vanishes at this order. Therefore after using the expansions in Eqs. (11)-(12), relations between phase shifts and T matrices of higher orders are

$$\delta^{(1)} = -k\bar{T}^{(1)} \quad (20)$$

$$\delta^{(2)} = -k\bar{T}^{(2)} - ik^2\bar{T}^{(1)2} \quad (21)$$

⋮

Note that the phase shift is real and there is no imaginary piece in Eq. (20). Also, the imaginary part of NNLO T matrix cancels the last term in Eq. (21). This is another way of checking the unitarity condition of the S matrix at each order in the perturbation.

A. The NLO and NNLO T matrices

In the three channels we consider in this paper, the T matrix and the renormalization procedure are independent of specific channel projections. Hence, at NLO there are OPE and dibaryon interactions shown in Fig. 1. The on-shell T matrix corresponding to these diagrams is

$$\bar{T}^{(1)}(k, m_\pi^2) = \bar{T}_\pi^{(1)}(k, m_\pi^2) + \frac{\eta m_N g_1^{(1)2} k^2}{k^2 - m_N \Delta^{(0)}}. \quad (22)$$

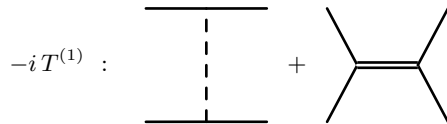


FIG. 1: Feynman diagrams corresponding to the NLO T matrix. The OPE potential contribution is shown on the left and the dibaryon contribution on the right. The nucleon-dibaryon coupling is $g_1^{(1)}$.

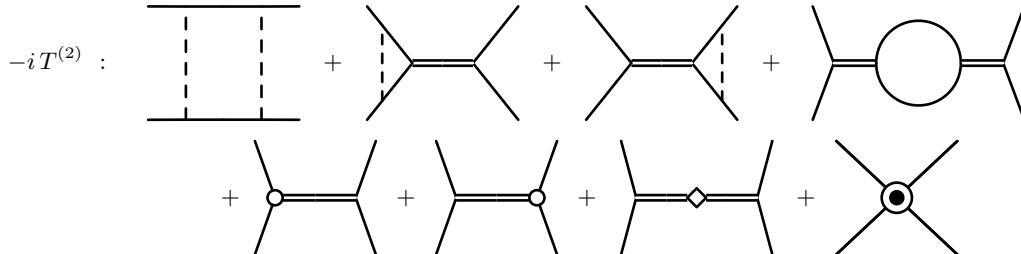


FIG. 2: Feynman diagrams corresponding to the NNLO T matrix. The first line involves NLO vertices and the second line involves NNLO vertices. The circle, diamond and double circle represent $\tilde{g}_1^{(2)}$, $\tilde{\Delta}^{(2)}$ and $C_2^{(2)}$ respectively.

where $\bar{T}_\pi^{(1)}(k, m_\pi^2)$, which is the on-shell tree level OPE T matrix for each channel, is given in the next section by taking the on-shell limit of the off-shell NLO T matrix in App. A.

The Feynman diagrams corresponding to the total NNLO T matrix are shown in Fig. 2. The two-pion ladder or box diagram is not divergent for the P waves, however the cross pion-dibaryon diagrams are linearly divergent (except for one channel), and the two-dibaryon diagram with a loop is divergent as well. While it is possible to derive analytic expressions of the divergent and pionless parts of the NNLO T matrix, we calculate the finite and real part of the first diagram in Fig. 2 numerically by the method described in the previous section⁵. The sum of the finite and real parts of the first three diagrams in Fig. 2 is

$$\mathcal{R}^{(2)}(k, g_1^{(1)}, \Delta^{(0)}, m_\pi^2) = \text{Re} \left[\bar{T}_{\pi\pi}^{(2)}(k, m_\pi) \right] + \frac{2\eta m_N g_1^{(1)2} k^2}{k^2 - m_N \Delta^{(0)}} \text{Re} \left[I_{\pi d}^{[\text{fin}]} \right], \quad (23)$$

where $\bar{T}_{\pi\pi}^{(2)}(k, m_\pi)$ is the on-shell T matrix of the box diagram from iteration of the OPE potential, and $I_{\pi d}^{[\text{fin}]}$ is the dimensionless finite part of the loop integral in the cross pion-dibaryon diagrams given in App. A. Then, the T matrix at NNLO can be expressed as

$$\begin{aligned} \bar{T}^{(2)}(k, m_\pi^2) = & -i k \left[\bar{T}^{(1)}(k, m_\pi^2) \right]^2 + \mathcal{R}^{(2)}(k, g_1^{(1)}, \Delta^{(0)}, m_\pi^2) + \frac{2\eta m_N g_1^{(1)2} k^2}{k^2 - m_N \Delta^{(0)}} \left[I_{\pi d}^{[\text{div}]} - \eta m_N g_1^{(1)2} \frac{L_1}{2} + \frac{\tilde{g}_1^{(2)}}{g_1^{(1)}} \right] \\ & + C_2^{(2)} k^2 - \frac{m_N^2 g_1^{(1)2} k^2}{(k^2 - m_N \Delta^{(0)})^2} \left[g_1^{(1)2} (L_3 + m_N \Delta^{(0)} L_1) - \eta \tilde{\Delta}^{(1)} \right], \end{aligned} \quad (24)$$

where $I_{\pi d}^{[\text{div}]}$ is the dimensionless divergent part of the loop integral in the cross pion-dibaryon diagrams given in App. A, and for a non-zero integer m and with a sharp-cutoff regulator, L_m is

$$L_m = \frac{2 \Lambda^m}{\pi m}. \quad (25)$$

⁵ An alternative numerical calculation of the box diagram from the OPE potential can be found in Ref. [31].

A few remarks: first, from Eqs.(A5)-(A7) in App. A $I_{\pi d}^{[\text{div}]}$ is not proportional to \bar{m}_π^2 , so there is no need for $D_4 m_\pi^2$ at NNLO, however the central values of the ‘‘chiral’’ NLO LECs will change due to the inclusion of $\omega_2^{(1)}$ and $h_3^{(2)}$ in $\tilde{\Delta}^{(1)}$ and $\tilde{g}_1^{(2)}$ respectively. But we can renormalize in a way that the central values of fitted chiral NLO plus CSB NNLO parameters stay unchanged. Second, all divergent terms in Eq. (24) can be absorbed by the NNLO expansions of NLO LECs, therefore $C_2^{(2)}$ is regulator independent. We find its value by fitting the result of the up-to-NNLO EFT phase shift to data. Finally, all imaginary parts of the NNLO T matrix come from diagrams in the first line of Fig. 2, and one can show numerically that their sum is the same as the imaginary term in Eq. (24), as is required by the unitarity condition of the S matrix.

To renormalize, we use a new method that keeps central fitted values of chiral NLO plus CSB NNLO parameters unchanged. There are two NLO LECs and two data points are needed at momenta $k = \{k_1, k_2\}$ to fix them. These fitted values are directly related to the experimental values or a model that describes the phase shift (like PWA) at those momenta. Therefore, in the up-to-NLO EFT we can attribute these fitted values to chiral parts, but at NNLO adding $\omega_2^{(1)}$ and $h_3^{(2)}$ means a portion of these fitted values are coming from CSB terms.

Since we want to keep the central values of the linear combination of chiral NLO and CSB NNLO terms unchanged at the momenta used in the NLO fit, the real part of the NNLO T matrix in Eq. (24) should contribute to the total up-to-NNLO T matrix ‘‘only’’ as a renormalized CSB value. Hence, we have

$$\text{Re} \left[\bar{T}^{(2)}(k_{1,2}, m_\pi^2) \right] = \frac{\eta m_N \gamma^{(2)} m_\pi^2 k_{1,2}^2}{k_{1,2}^2 - m_N \Delta^{(0)}} + \frac{\eta m_N^2 g_1^{(1)2} \theta^{(1)} m_\pi^2 k_{1,2}^2}{(k_{1,2}^2 - m_N \Delta^{(0)})^2}, \quad (26)$$

where $\theta^{(1)}$ and $\gamma^{(2)}$ are renormalized values related to $\omega_2^{(1)}$ and $h_3^{(2)}$ respectively. The above equation is an abbreviation for two conditions⁶ at k_1 and k_2 . From these two conditions, we can find $\tilde{g}_1^{(2)}$ and $\tilde{\Delta}^{(1)}$, given in App. A, in terms of NLO fitted values, the cutoff Λ , $C_2^{(2)}$ and complicated nonanalytic functions of m_π [14, 34]. With the conditions in Eq. (26), the renormalized NNLO T matrix is

$$\begin{aligned} \bar{T}^{(2)}(k, m_\pi^2) &= -ik \left[\bar{T}^{(1)}(k, m_\pi^2) \right]^2 + \frac{\eta m_N \gamma^{(2)} m_\pi^2 k^2}{k^2 - m_N \Delta^{(0)}} + \frac{\eta m_N^2 g_1^{(1)2} \theta^{(1)} m_\pi^2 k^2}{(k^2 - m_N \Delta^{(0)})^2} + \mathcal{R}^{(2)}(k, g_1^{(1)}, \Delta^{(0)}, m_\pi^2) \\ &\quad - \frac{(k^2 - k_2^2)(k_1^2 - m_N \Delta^{(0)})^2 k^2}{(k_1^2 - k_2^2)(k^2 - m_N \Delta^{(0)})^2 k_1^2} \mathcal{R}_{k_1}^{(2)} + \frac{(k^2 - k_1^2)(k_2^2 - m_N \Delta^{(0)})^2 k^2}{(k_1^2 - k_2^2)(k^2 - m_N \Delta^{(0)})^2 k_2^2} \mathcal{R}_{k_2}^{(2)} \\ &\quad + \frac{(k^2 - k_1^2)(k^2 - k_2^2)}{(k^2 - m_N \Delta^{(0)})^2} C_2^{(2)} k^2, \end{aligned} \quad (27)$$

with $\mathcal{R}_{k_{1,2}}^{(2)} \equiv \mathcal{R}^{(2)}(k_{1,2}, g_1^{(1)}, \Delta^{(0)}, m_\pi^2)$. The total phase shift up to NNLO from Eqs. (20)-(21) is

$$\begin{aligned} -\frac{\delta^{(t)}}{k} &= -\frac{1}{k} (\delta^{(1)} + \delta^{(2)}) = \bar{T}_\pi^{(1)}(k, m_\pi^2) + \frac{\eta m_N \bar{g}_1^{(1)2} k^2}{k^2 - m_N \Delta^{(0)}} + \mathcal{R}^{(2)}(k, g_1^{(1)}, \Delta^{(0)}, m_\pi^2) + \frac{(k^2 - k_1^2)(k^2 - k_2^2)}{(k^2 - m_N \Delta^{(0)})^2} C_2^{(2)} k^2 \\ &\quad - \frac{(k^2 - k_2^2)(k_1^2 - m_N \Delta^{(0)})^2 k^2}{(k_1^2 - k_2^2)(k^2 - m_N \Delta^{(0)})^2 k_1^2} \mathcal{R}_{k_1}^{(2)} + \frac{(k^2 - k_1^2)(k_2^2 - m_N \Delta^{(0)})^2 k^2}{(k_1^2 - k_2^2)(k^2 - m_N \Delta^{(0)})^2 k_2^2} \mathcal{R}_{k_2}^{(2)}, \end{aligned} \quad (28)$$

where the finite $\bar{\Delta}^{(0)}$ and $\bar{g}_1^{(1)2}$ are

$$\bar{\Delta}^{(0)} \equiv \Delta^{(0)} + \theta^{(1)} m_\pi^2, \quad (29)$$

$$\bar{g}_1^{(1)2} \equiv g_1^{(1)2} + \gamma^{(2)} m_\pi^2. \quad (30)$$

⁶ In a pionless theory, the right hand side of Eq. (26) is zero which is similar to conditions put on pionless theories by keeping the experimental values of the effective range parameters fixed.

This method of renormalization uses data points instead of an interval of data, so the number of data points we need at each order in the perturbation is equivalent to the number of new LECs at that order. For example, at NLO we have two LECs and two data points are needed at $k = \{k_1, k_2\}$. At NNLO in principle we need three additional data points to determine $\theta^{(1)}$, $\gamma^{(2)}$ and $C_2^{(2)}$, however as we can see in Eqs. (29)-(30) it is impossible to distinguish between chiral and CSB fitting parameters from one scattering process with a fixed value of m_π^2 . Therefore, we only need one more data point at $k = k_3$ to determine only $C_2^{(2)}$, and the central values of $\bar{\Delta}^{(0)}$ and $\bar{g}_1^{(1)2}$ are kept fixed to the NLO fitted values.

Note that keeping the NLO fitted values fixed does not mean that $\bar{\Delta}^{(0)} = \Delta^{(0)}$ or $\bar{g}_1^{(1)2} = g_1^{(1)2}$. It means that the main portion of the actual values that we fit at NLO are chiral, and a small and perturbative part of them are due to CSB parts, which we could not resolve at NLO. At NNLO, however, the effect of these CSB parts becomes manifest to order m_π^2 , and they can be distinguished via $\theta^{(1)}$ and $\gamma^{(2)}$, although the combinations with the chiral parts still have the same fitted values as at NLO. In order to find the values for $\theta^{(1)}$ and $\gamma^{(2)}$ we need new data points taken either from lattice calculations of the same process with a different value of m_π^2 or another m_π -sensitive process. Since $\Delta^{(0)}$ and $g_1^{(1)2}$ in Eq. (28) appear in NNLO terms, we can replace them with $\bar{\Delta}^{(0)}$ and $\bar{g}_1^{(1)2}$ and use the same fitted NLO values when we fit the total phase shift to data. A different method of renormalization is explained in App. B.

The forms of the last three terms in Eq. (28) are specific combinations of terms in Eq. (24). Although these forms ensure that the two conditions in Eq. (26) are fulfilled, their overall effect is more than just that. They counteract effects of nonanalytic terms in pion interactions that arise in $\mathcal{R}^{(2)}(k, g_1^{(1)}, \Delta^{(0)}, m_\pi^2)$. It is remarkable that simple functions like these rectify the effects of a complicated function like $\mathcal{R}^{(2)}$ in almost the entire region of validity of the EFT.

IV. RESULTS

In order to fit EFT results, we need three data points for the three LECs Δ , g_1 and C_2 . The higher order contributions to these LECs do not change the number of parameters we need to determine. We choose two sets of data points for each channel in order to show that final results have not been optimized by a specific choice of momenta. Since $\Delta^{(0)}$, $g_1^{(1)}$ and $C_2^{(2)}$ are finite, we estimate their order of magnitude according to the PC and the size of $M_{lo} \sim 300$ MeV and $M_{hi} \sim 1$ GeV

$$\begin{aligned} \sqrt{m_N \Delta^{(0)}} &\sim M_{lo} \sim 300 \text{ MeV} \\ g_1^{(1)} &\sim \frac{1}{M_{hi}} \sim 10^{-3} \text{ MeV}^{-1} \\ C_2^{(2)} &\sim \frac{1}{M_{lo} M_{hi}^2} \sim 10^{-9} - 10^{-8} \text{ MeV}^{-3}. \end{aligned} \quad (31)$$

In order to get the values of $\Delta^{(0)}$ and $g_1^{(1)}$, we choose two momenta that give the best fit to data. For the third data point needed for $C_2^{(2)}$, we have more freedom, so we can choose a data point which gives the best result at NNLO. The total up-to-NNLO EFT phase shift is given in Eq. (28), and for the fit we use the phase shift from the Nijmegen PWA [26, 27] for lab energies $E_{lab} \leq 350$ MeV.

As has been shown by Fleming *et al.* [12, 13] and Pavón Valderrama *et al.* [35], while the phase shift from iterating the OPE potential in the 1P_1 channel converges quickly, it does a poor job of describing the data above the pion mass. Adding a dibaryon field goes a long way in solving the convergence-to-data problem. The on-shell T matrix in the 1P_1 channel at NLO is (see App. A)

$$\bar{T}^{(1)({}^1P_1)}(k, m_\pi^2) = \frac{\eta m_N g_1^{(1)2} k^2}{k^2 - m_N \Delta^{(0)}} + \frac{1}{\Lambda_{NN}} \left[-\frac{3 m_\pi^2}{2 k^2} + \frac{3 m_\pi^2 (m_\pi^2 + 2 k^2)}{8 k^4} \ln \left(1 + \frac{4 k^2}{m_\pi^2} \right) \right]. \quad (32)$$

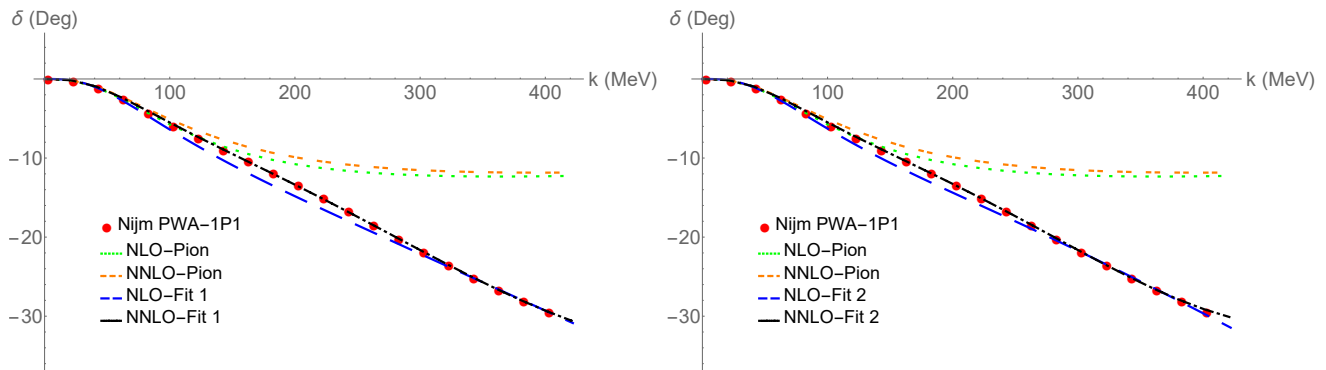


FIG. 3: The Nijmegen PWA (red circles) vs NLO (blue long-dashed line) and NNLO (black short-dashed line) EFT results for the 1P_1 channel. Also shown are the results from pion only contributions, which represent the KSW PC, at NLO (green dotted line) and NNLO (orange double-dotted line). We use the momentum sets given in Table. I for fitting and graph the results on the left for fit 1, and on the right for fit 2.

1P_1	$\{k_1, k_2, k_3\}(\text{MeV})$	$g_1^{(1)} (\text{MeV}^{-1})$	$\Delta^{(0)} (\text{MeV})$	$C_2^{(2)} (\text{MeV}^{-3})$	$\sqrt{m_N \Delta^{(0)} } (\text{MeV})$	η
Fit 1	350, 400, 300	0.00112	-97.8	-3.8×10^{-9}	303.0	+1
Fit 2	310, 370, 280	0.00123	-149.2	-7.7×10^{-9}	374.3	+1

TABLE I: Results of fitting the up-to-NNLO LECs in the 1P_1 channel to the Nijmegen PWA phase shift for two sets of data points at momenta $\{k_1, k_2, k_3\}$. After fitting the NLO constants $g_1^{(1)}$ and $\Delta^{(0)}$ to the data points $\{k_1, k_2\}$, k_3 fixes the $C_2^{(2)}$ at NNLO. Note that the fitted value of $\bar{\Delta}^{(0)}$ at NNLO is the same as the fitted value of $\Delta^{(0)}$ at NLO.

The Results of fitting the T matrix to two data points $\{k_1, k_2\}$ are given in Table. I and the corresponding phase shift is plotted in Fig. 3 (blue long-dashed lines). Even at NLO, an improvement relative to perturbative OPE potential for momenta above $k \sim 200$ MeV is evident. We use Eq. (23) and Eq. (27) to fit the NNLO EFT calculated phase shift to the Nijmegen PWA at the third data point, $k = k_3$. The results are given in Table. I and plotted in Fig. 3 (black short-dashed lines). Clearly the NNLO results are in an even better agreement with data than those at NLO.

Another way of checking the PC is by looking at the fitted finite values of LECs. The size of fitted parameters in Table. I are close to the estimation from the PC in Eq. (31). With a negative $\Delta^{(0)}$, the denominator of the NLO T matrix vanishes for an imaginary momentum $\sqrt{m_N |\Delta^{(0)}|}$. This imaginary momentum cannot be an “imaginary” pole corresponding to a bound/virtual state, because around such a pole the phase shift experiences large changes of order $\pi/2$. In terms of EFT, an imaginary pole appears when there is a resummation in loop integrals and the unitary part of the loop integrals are on equal footing to the imaginary pole, which is not the case here either. It is possible that this imaginary momentum corresponds to an imaginary zero of amplitude, which is not visible in the real phase shift or in $k \cot \delta$.

The interesting $k^2 \gg m_N \Delta^{(0)}, m_\pi^2$ limit of the LO T matrix is

$$\lim_{k^2 \gg m_N \Delta^{(0)}, m_\pi^2} \bar{T}^{(1)(^1P_1)} = \eta m_N g_1^{(1)2} + \dots, \quad (33)$$

where $\eta = +1$ for this channel means the phase shift in Eq. (20) decreases linearly at larger momenta. This is a feature coming from the dibaryon field, not the contact interactions. The same feature holds for the 3P_0 and 3P_1 channels too.

The lower spin-triplet channels are real challenges for the KSW PC at NNLO because of the large disagreement with data [12]. These channels have thus been the subject of many studies, for example see [25, 36–40]. The 3P_0 channel is a special case because unlike the other uncoupled P -wave channels its phase shift does not decrease or

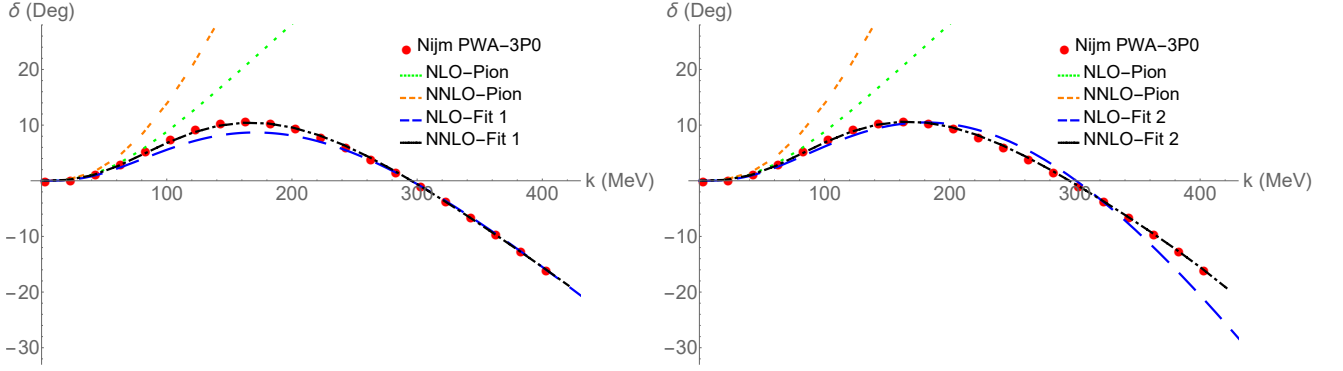


FIG. 4: The 3P_0 channel results for momentum sets of fit 1 (left) and fit 2 (right) in Table. II. For notation and explanation see Fig. 3.

3P_0	$\{k_1, k_2, k_3\}$ (MeV)	$g_1^{(1)}$ (MeV $^{-1}$)	$\Delta^{(0)}$ (MeV)	$C_2^{(2)}$ (MeV $^{-3}$)	$\sqrt{m_N \Delta^{(0)} }$ (MeV)	η
Fit 1	300, 400, 200	0.00250	-99.7	1.2×10^{-8}	305.9	+1
Fit 2	180, 320, 380	0.00286	-168.0	2.6×10^{-8}	397.2	+1

TABLE II: Results for fitting up-to-NNLO LECs in the 3P_0 channel. For notation and explanation see Table. I.

increase monotonically and it passes zero at $k \sim 300$ MeV similar to the 1S_0 channel. In contrast however, the overall size of the phase shift is not large enough to support the idea of a pole in the T matrix.

For the 3P_0 channel, the total on-shell T matrix at NLO can be extracted from the off-shell T matrix in the diagrams in Fig. 1 (see App. A)

$$\bar{T}^{(1)({}^3P_0)}(k, m_\pi^2) = \frac{\eta m_N g_1^{(1)2} k^2}{k^2 - m_N \Delta^{(0)}} + \frac{1}{\Lambda_{NN}} \left[-1 + \frac{m_\pi^2}{4k^2} \ln \left(1 + \frac{4k^2}{m_\pi^2} \right) \right]. \quad (34)$$

The k^2 term in the numerator of dibaryon part is due to the P -wave nature of this channel. In the denominator, when k^2 is small relative to $m_N \Delta^{(0)}$ an expansion of the dibaryon propagator is similar to the on-shell contact interactions in Ref. [25].

Fitted values of $g_1^{(1)}$, $\Delta^{(0)}$ and $C_2^{(2)}$ from two sets of momenta are given in Table. II and the phase shift is plotted in Fig. 4. As we see from the graphs, the importance of the dibaryon field shows itself in the $k^2 \gg m_N \Delta^{(0)}$, m_π^2 limit where the T matrix is a constant at this order

$$\lim_{k^2 \gg m_N \Delta^{(0)}, m_\pi^2} \bar{T}^{(1)({}^3P_0)} = -\frac{1}{\Lambda_{NN}} + \eta m_N g_1^{(1)2} + \dots \quad (35)$$

One can check that with $\eta = +1$ and the fitted values of parameters in Table. II, the sum of the first two terms is positive. Therefore the phase shift decreases linearly at larger momenta, in contrast to the quadratic behavior due to the contact term $C_2 k^2$ [25].

Again, fitted values for this channel are close to the estimation of the PC. The NLO EFT phase shift shows real improvement relative to the results of the KSW PC for momenta below $k \sim 200$ MeV, and the agreement with data improves at NNLO. Similar to the 1P_1 channel, there is a possible imaginary zero in the denominator of the T matrix in the 3P_0 channel.

In the KSW PC there are no new parameters at NNLO in the P -wave channels, therefore these channels are good benchmarks to test the convergence of the theory. For the 3P_1 channel, the phase shifts at NLO and NNLO agree well with data only up to $k \sim 200$ MeV. This is evidence that pion interactions alone are not enough to get good agreement with data in a perturbative EFT for typical momenta about 300 MeV. Alternative options are to either

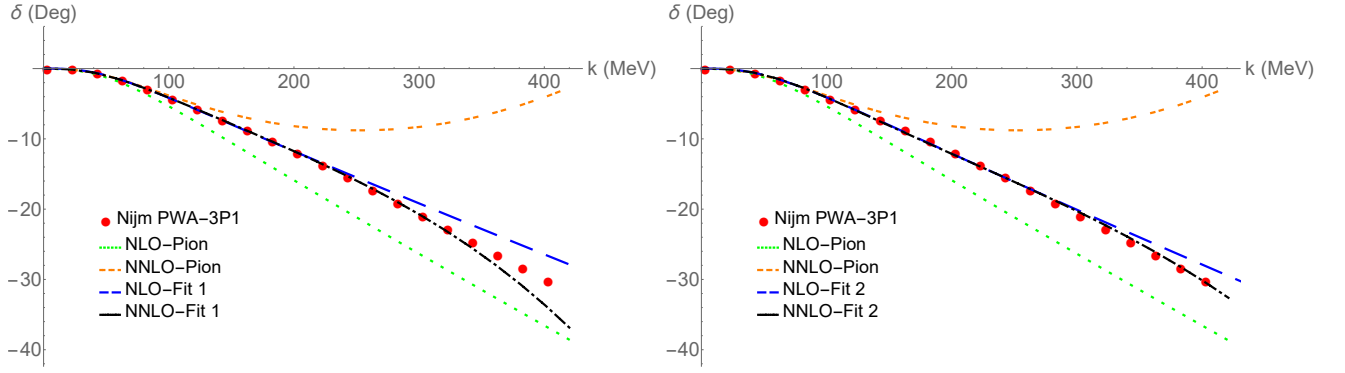


FIG. 5: The 3P_1 channel results for momentum sets of fit 1 (left) and fit 2 (right) in Table. III. For notation and explanation see Fig. 3.

3P_1	$\{k_1, k_2, k_3\}$ (MeV)	$g_1^{(1)}$ (MeV $^{-1}$)	$\Delta^{(0)}$ (MeV)	$C_2^{(2)}$ (MeV $^{-3}$)	$\sqrt{m_N \Delta^{(0)} }$ (MeV)	η
Fit 1	60, 200, 300	0.00071	-13.8	7.9×10^{-9}	114.0	-1
Fit 2	100, 250, 390	0.00065	-8.7	5.9×10^{-9}	90.4	-1

TABLE III: Results for fitting up-to-NNLO LECs in the 3P_1 channel. For notation and explanation see Table. I.

include additional contact interactions or a dibaryon field. In this paper we consider the later. The on-shell NLO T matrix in the 3P_1 channel is (see App. A)

$$\bar{T}^{(1)({}^3P_1)}(k, m_\pi^2) = \frac{\eta m_N g_1^{(1)2} k^2}{k^2 - m_N \Delta^{(0)}} + \frac{1}{\Lambda_{NN}} \left[\frac{2k^2 - m_\pi^2}{4k^2} + \frac{m_\pi^4}{16k^4} \ln \left(1 + \frac{4k^2}{m_\pi^2} \right) \right]. \quad (36)$$

Fitted values of the LECs are given in Table. III, and the phase shift is plotted in Fig. 5.

Since $\Delta^{(0)} < 0$, there is a possible imaginary zero in this channel too, although unlike the other two channels $\eta = -1$. Again, the size of the fitted parameters is of the same order as the estimation from the PC. In Fig. 5 we see good agreement at NLO, which further improves at NNLO. Note that this happens because the dibaryon field cancels the large upturn due to the OPE box diagram in this channel. The large- k limit of NLO T matrix for this channel is

$$\lim_{k^2 \gg m_N \Delta^{(0)}, m_\pi^2} \bar{T}^{(1)({}^3P_1)} = \frac{1}{2\Lambda_{NN}} + \eta m_N g_1^{(1)2} + \dots, \quad (37)$$

and with the fitted parameters in Table. II, it is positive up to the first two terms. Again this shows that phase shift decreases linearly for large momenta in this channel too.

V. CONCLUSION

A new EFT including a dibaryon field with perturbative pions is investigated for the uncoupled P -wave channels of nucleon-nucleon scattering systems, and promising results up to NNLO are observed. This is (strong) evidence that to have a convergent perturbative EFT beyond the pion mass [14], physics of higher energies has to be included by introducing an auxiliary dibaryon field to make pion interactions perturbative. The PC for chiral contact LECs in this theory are the same as NDA [10, 11], and the PC for CSB contact interactions in Eq. (2) has been adapted from the KSW PC and NDA. The PC for the chiral and CSB dibaryon LECs in Eqs. (3)-(4) show that dibaryon interactions start perturbatively at NLO.

Calculations are carried out up to NNLO for the selected P -wave channels with a new method that combines renormalization and fitting together. All pionless and related-to-dibaryon parts of diagrams are calculated analytically,

although the finite part of the box diagram from iteration of the OPE potential is done numerically. No m_π^2 -dependence has been observed in divergent parts, therefore there is no need to add CSB “contact” counter terms at NNLO. The CSB dibaryon LECs, however, start to appear at NNLO which absorb the effect of nonanalytic terms proportional to m_π^2 coming from the iteration of the OPE potential. Since LECs at NLO and the new $C_2^{(2)}$ at NNLO have fixed values which do not run with the regulator, their sizes are estimated by the new PC in Eq. (31). According to the results given in Tables. I, II and III, fitted values of LECs are in good agreement with those estimated by PC. The renormalization method in Sec. III is new and useful for numerical calculations, which uses data points instead of an interval of data. Furthermore it produces renormalized parts that counteract the effect of nonanalytic terms coming from pion interactions. In App. B, the theory has been renormalized by using the usual method in the literature of nuclear EFTs, so one can compare results in both renormalization methods.

An advantage of including the dibaryon at NLO, instead of using contact interactions, is that the tree level T matrix of the dibaryon is a constant in the large- k limit ($k^2 \gg m_N \Delta^{(0)}, m_\pi^2$) as can be seen from Eqs. (20), (33), (35) and (37). This means the phase shift at NLO has a linear behavior in this limit which is also noticeable in the Nijmegen PWA of these channels for larger momenta below the mass of ρ meson.

These promising results for the uncoupled P -wave channels are encouraging, and motivate the application of the same idea to the $^1S_0, ^3S_1 - ^3D_1, ^3P_2 - ^3F_2$ and higher partial wave channels. The S -wave channels are more challenging than others, because they have a non-zero LO T matrix from the resummation of $C_0^{(0)}$. Preliminary NLO calculations for higher partial wave channels also show promising results, although before carrying out NNLO calculations in those channels we cannot draw solid conclusions yet.

Acknowledgments

I would like to thank S. Fleming and U. van Kolck for their encouragement and valuable supports, useful discussions about renormalization and thoughtful comments on the manuscript. This research was supported in part by the U.S. Department of Energy, Office of Science, Office of Nuclear Physics, under award number DE-FG02-04ER41338.

Appendix A: Ingredients for T matrix calculations

One can drive the off-shell tree level pion and dibaryon diagrams by using the trace technique explained in Ref. [12]. For the $^1P_1, ^3P_0$ and 3P_1 channels we get

$$\bar{T}_\pi^{(1)(^1P_1)}(p', p, k, m_\pi^2) = \frac{1}{\Lambda_{NN}} \left[-\frac{3m_\pi^2}{2pp'} + \frac{3m_\pi^2(m_\pi^2 + p^2 + p'^2)}{8p^2p'^2} \ln \left(\frac{m_\pi^2 + (p+p')^2}{m_\pi^2 + (p-p')^2} \right) \right], \quad (\text{A1})$$

$$\bar{T}_\pi^{(1)(^3P_0)}(p', p, k, m_\pi^2) = \frac{1}{\Lambda_{NN}} \left[-\frac{1}{2pp'}(p^2 + p'^2) + \frac{m_\pi^2(p^2 + p'^2) + (p^2 - p'^2)^2}{8p^2p'^2} \ln \left(\frac{m_\pi^2 + (p+p')^2}{m_\pi^2 + (p-p')^2} \right) \right], \quad (\text{A2})$$

$$\bar{T}_\pi^{(1)(^3P_1)}(p', p, k, m_\pi^2) = \frac{1}{\Lambda_{NN}} \left[\frac{1}{4pp'}(p^2 + p'^2 - m_\pi^2) + \frac{m_\pi^4 - (p^2 - p'^2)^2}{16p^2p'^2} \ln \left(\frac{m_\pi^2 + (p+p')^2}{m_\pi^2 + (p-p')^2} \right) \right], \quad (\text{A3})$$

$$\bar{T}_d^{(1)(s)}(p', p, k) = \frac{\eta^{(s)} m_N g_1^{(1)(s)^2} pp'}{k^2 - m_N \Delta^{(0)(s)}}. \quad (\text{A4})$$

The structure of the dibaryon parts of off-shell T matrices are the same, but with different LECs. One can check that on-shell pion T -matrices are the same as those in Ref. [12]. Also the numerical calculation of the T matrix for the box diagram of OPE potential by using the above off-shell T matrices and Eq. (18) agrees with the results in Ref. [31].

After inserting the various contributions of the off-shell T matrix in the projected LSE in Eq. (18), we use contour integration to find divergent and finite parts of loop integrals. If we define the dimensionless loop integral as $I_{\pi d} =$

$I_{\pi d}^{[\text{div}]} + I_{\pi d}^{[\text{fin}]}$, we get

$$I_{\pi d}^{(1P_1)} = \frac{3 m_\pi^2}{2 \Lambda_{NN} k^2} \left[m_\pi - k \left(1 + \frac{m_\pi^2}{2k^2} \right) \tan^{-1} \left(\frac{2k}{m_\pi} \right) \right] + \frac{3 i m_\pi^2}{2 \Lambda_{NN} k} \left[1 - \left(\frac{1}{2} + \frac{m_\pi^2}{4k^2} \right) \ln \left(1 + \frac{4k^2}{m_\pi^2} \right) \right] \quad (\text{A5})$$

$$I_{\pi d}^{(3P_0)} = \frac{4 L_1}{3 \Lambda_{NN}} - \frac{m_\pi^2}{2 \Lambda_{NN} k} \tan^{-1} \left(\frac{2k}{m_\pi} \right) + \frac{i k}{\Lambda_{NN}} \left[1 - \frac{m_\pi^2}{4k^2} \ln \left(1 + \frac{4k^2}{m_\pi^2} \right) \right] \quad (\text{A6})$$

$$I_{\pi d}^{(3P_1)} = -\frac{2 L_1}{3 \Lambda_{NN}} + \frac{m_\pi^3}{4 \Lambda_{NN} k^2} \left[1 - \frac{m_\pi}{2k} \tan^{-1} \left(\frac{2k}{m_\pi} \right) \right] + \frac{i}{2 \Lambda_{NN} k} \left[\frac{m_\pi^2}{2} - k^2 - \frac{m_\pi^4}{8k^2} \ln \left(1 + \frac{4k^2}{m_\pi^2} \right) \right] \quad (\text{A7})$$

where L_m are given in Eq. (25). It is interesting that in the 1P_1 channel the cross pion-dibaryon loop integral does not contain a divergent term, although from a naive counting we expect the opposite. The reason is the cancellation among integrand terms in the on-shell NNLO T matrix. As we can see in above equations, real and finite parts of pion-dibaryon loop integrals are complicated functions of k/m_π and also contain odd powers of m_π and negative powers of k . There are no terms in the Lagrangian with odd powers of m_π or negative powers of k , therefore we absorb the effects of these nonanalytic terms at specific momenta into the same order LECs in the renormalization step (see Sec. III). Another approach is to absorb effects of these terms into a redefinition of NLO LECs during fitting (see App. B).

The running of the NNLO contributions of NLO LECs in Sec. III with regulator Λ is given by

$$\begin{aligned} \tilde{\Delta}^{(1)} &= \Delta^{(1)} + \omega_2^{(1)} m_\pi^2 \\ &= \eta g_1^{(1)2} \left(L_3 + m_N \Delta^{(0)} L_1 \right) + \theta^{(1)} m_\pi^2 + \frac{(k_1^2 - m_N \Delta^{(0)}) (k_2^2 - m_N \Delta^{(0)})}{g_1^{(1)2} m_N^2} \eta C_2^{(2)} \\ &\quad + \frac{(k_1^2 - m_N \Delta^{(0)})^2 (k_2^2 - m_N \Delta^{(0)})}{g_1^{(1)2} m_N^2 k_1^2 (k_1^2 - k_2^2)} \eta \mathcal{R}_{k_1}^{(2)} - \frac{(k_1^2 - m_N \Delta^{(0)}) (k_2^2 - m_N \Delta^{(0)})^2}{g_1^{(1)2} m_N^2 k_2^2 (k_1^2 - k_2^2)} \eta \mathcal{R}_{k_2}^{(2)}, \end{aligned} \quad (\text{A8})$$

$$\begin{aligned} \tilde{g}_1^{(2)} &= g_1^{(2)} + h_3^{(2)} m_\pi^2 \\ &= \frac{\eta}{2} g_1^{(1)3} m_N L_1 - g_1^{(1)} I_{\pi d}^{[\text{div}]} + \frac{\gamma^{(2)} m_\pi^2}{2 g_1^{(1)}} + \frac{2 m_N \Delta^{(0)} - (k_1^2 + k_2^2)}{2 g_1^{(1)} m_N} \eta C_2^{(2)} \\ &\quad - \frac{(k_1^2 - m_N \Delta^{(0)})^2}{2 g_1^{(1)} m_N k_1^2 (k_1^2 - k_2^2)} \eta \mathcal{R}_{k_1}^{(2)} + \frac{(k_2^2 - m_N \Delta^{(0)})^2}{2 g_1^{(1)} m_N k_2^2 (k_1^2 - k_2^2)} \eta \mathcal{R}_{k_2}^{(2)}, \end{aligned} \quad (\text{A9})$$

where values of $\Delta^{(0)}$, $g_1^{(1)}$ and $C_2^{(2)}$ are the fitted values in the tables. The $\mathcal{R}_{k_{1,2}}^{(2)} \equiv \mathcal{R}^{(2)}(k_{1,2}, g_1^{(1)}, \Delta^{(0)}, m_\pi^2)$ functions contain chiral and CSB parts, therefore all the chiral terms of right hand sides in above equations will define $\Delta^{(1)}$ and $g_1^{(2)}$. Also, all CSB parts will define $\omega_2^{(1)} m_\pi^2$ and $h_3^{(2)} m_\pi^2$. We know that these chiral and CSB LECs absorb nonanalytic parts coming from $\mathcal{R}_{k_{1,2}}^{(2)}$ [14, 34].

Appendix B: The Second Method of Renormalization

We can renormalize by not absorbing nonanalytic functions of m_π into the NNLO LECs [6, 7, 12, 41]. By setting square bracket terms in Eq. (24) equal to the same form as the right hand side of Eq. (26) for a general k instead of $k_{1,2}$, the NNLO T matrix is

$$\begin{aligned} \bar{T}^{(2)}(k, m_\pi^2) &= -i k \left[\bar{T}^{(1)}(k, m_\pi^2) \right]^2 + \frac{\eta m_N \gamma^{(2)} m_\pi^2 k^2}{k^2 - m_N \Delta^{(0)}} + \frac{\eta m_N^2 g_1^{(1)2} \theta^{(1)} m_\pi^2 k^2}{(k^2 - m_N \Delta^{(0)})^2} + C_2^{(2)} k^2 \\ &\quad + \mathcal{R}^{(2)}(k, g_1^{(1)}, \Delta^{(0)}, m_\pi^2). \end{aligned} \quad (\text{B1})$$

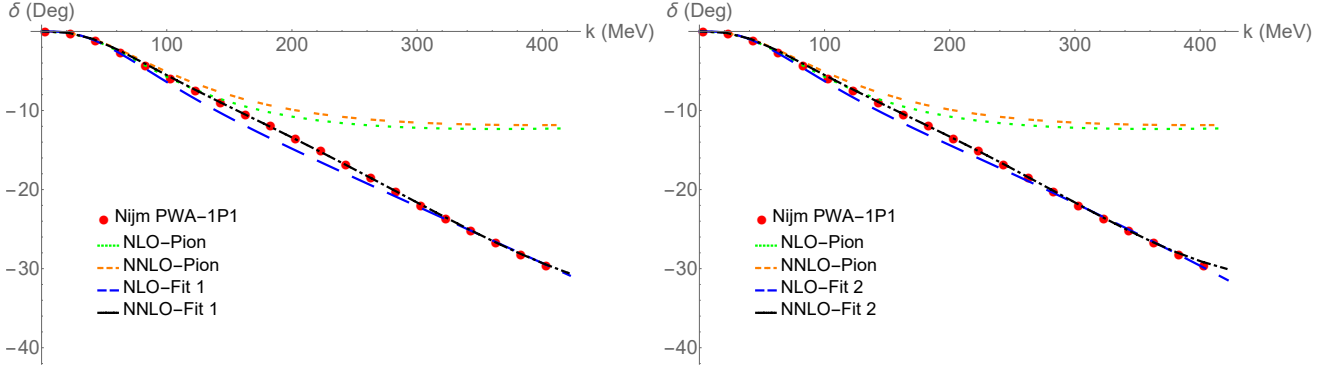


FIG. 6: The 1P_1 channel results from an alternative method of renormalization for momentum sets of fit 1 (left) and fit 2 (right) in Table. IV. For notation and explanation see Fig. 3.

1P_1	$\{k_1, k_2, k_3\}$	$g_1^{(1)}$	$\bar{g}_1^{(1)}$	$\%g_1^{(1)}$	$\Delta^{(0)}$	$\bar{\Delta}^{(0)}$	$\%\Delta^{(0)}$	$C_2^{(2)}$	$\sqrt{m_N \Delta^{(0)} }$	$\sqrt{m_N \bar{\Delta}^{(0)} }$	η
Fit 1	350, 400, 300	0.00112	0.00195	% 74.6	-97.8	-153.2	% 56.7	-4.3×10^{-9}	303.0	379.2	+1
Fit 2	310, 370, 280	0.00123	0.00292	% 137.8	-149.2	-304.9	% 104.3	-1.1×10^{-8}	374.3	535.0	+1

TABLE IV: Results for fitting up-to-NNLO LECs of the 1P_1 channel with the alternative method of renormalization. We re-fit the total LECs given in Eqs. (29)-(30) with the same momentum sets. The $\%g_1^{(1)}$ and $\%\Delta^{(0)}$ give the percentage of change relative to NLO values after re-fitting. The units are the same as Table. I.

The bare NNLO LECs are given by Eqs. (A8)-(A9), after removing terms containing $C_2^{(2)}$ and $\mathcal{R}_{k_{1,2}}^{(2)}$. The total up-to-NNLO phase shift also has a new form

$$-\frac{\delta^{(t)}}{k} = -\frac{1}{k}(\delta^{(1)} + \delta^{(2)}) = \bar{T}_\pi^{(1)}(k, m_\pi^2) + \frac{\eta m_N \bar{g}_1^{(1)2} k^2}{k^2 - m_N \bar{\Delta}^{(0)}} + C_2^{(2)} k^2 + \mathcal{R}^{(2)}(k, g_1^{(1)}, \Delta^{(0)}, m_\pi^2), \quad (\text{B2})$$

where the $\bar{\Delta}^{(0)}$ and $\bar{g}_1^{(1)2}$ are given in Eqs. (29)-(30). The chiral part of NNLO T matrix does not vanish at $k = k_1, k_2$, therefore unlike the previous method of renormalization we let $\bar{\Delta}^{(0)}$ and $\bar{g}_1^{(1)2}$ change when fitting at NNLO. We use the NLO fitted values of $\Delta^{(0)}$ and $g_1^{(1)2}$ in the NNLO part of the phase shift, and $\bar{\Delta}^{(0)}$ and $\bar{g}_1^{(1)2}$ are used in the NLO part only. Since there are nonanalytic terms we cannot predict the effects of these terms on re-fitted LECs because $Q \sim k \sim m_\pi \sim \Lambda_{NN}$. These effects can be small or large relative to NLO values, but the only thing that we expect is that even re-fitted values are within the estimation of the PC in Eq. (31).

The results for 1P_1 and 3P_0 channels are given in Tables. IV and V and plots of the phase shift are shown in Figs. 6 and 7, respectively. In the 3P_1 channel the error introduced by using data points is too high which makes it hard to find reasonable re-fitted values. For this case, it is better to use an interval of data and for that an analytical expression of $\mathcal{R}^{(2)}(k, g_1^{(1)}, \Delta^{(0)}, m_\pi^2)$ is preferable.

As we can see in Tables. IV and V, effects of nonanalytic terms that have been absorbed in re-fitted values are not perturbative and small relative to NLO fitted values, although generally the results at NNLO are in better agreement with data than at NLO. As we expected, re-fitted values are also within the estimation of PC in Eq. (31).

Note that our goal is not to find a PC in which contributions from the OPE potential are small, therefore it is not appropriate to conclude from the large shift in the fitted values of LECs going from NLO to NNLO that perturbation theory breaks down. Our goal is to make the effects of pion interactions perturbative by using the dibaryon field and indeed this is happening in the first method of renormalization. In the first method, however, we cannot find the

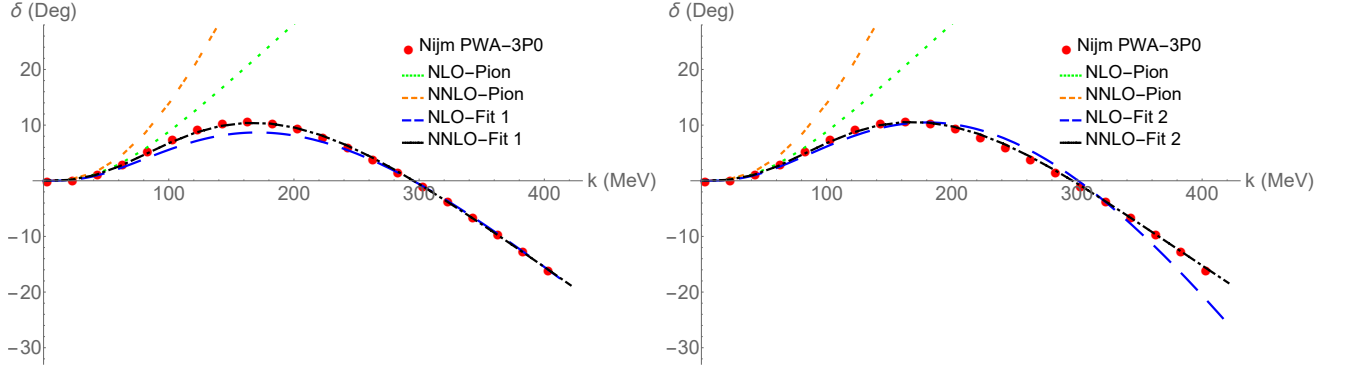


FIG. 7: The 3P_0 channel results from an alternative method of renormalization for momentum sets of fit 1 (left) and fit 2 (right) in Table. V. For notation and explanation see Fig. 3.

3P_0	$\{k_1, k_2, k_3\}$	$g_1^{(1)}$	$\bar{g}_1^{(1)}$	$\% g_1^{(1)}$	$\Delta^{(0)}$	$\bar{\Delta}^{(0)}$	$\% \Delta^{(0)}$	$C_2^{(2)}$	$\sqrt{m_N \Delta^{(0)} }$	$\sqrt{m_N \bar{\Delta}^{(0)} }$	η
Fit 1	300, 400, 200	0.00250	0.00359	% 44.0	-99.7	-75.6	% 24.2	1.0×10^{-8}	305.9	266.4	+1
Fit 2	180, 320, 380	0.00286	0.00373	% 29.6	-168.0	-85.5	% 49.1	8.5×10^{-9}	397.2	283.3	+1

TABLE V: Results for fitting up-to-NNLO LECs of the 3P_0 channel with the alternative method of doing renormalization. For units, notation and explanation see Table. IV.

change to the fitted NLO parameters until we know the values of $\gamma^{(2)}$ and $\theta^{(1)}$.

-
- [1] S. Weinberg, Phys. Lett. B **251** (1990) 288.
 - [2] S. Weinberg, Nucl. Phys. B **363** (1991) 3.
 - [3] C. Ordonez and U. van Kolck, Phys. Lett. B **291**, 459-464 (1992)
 - [4] C. Ordonez, L. Ray and U. van Kolck, Phys. Rev. Lett. **72**, 1982-1985 (1994)
 - [5] D.B. Kaplan, M.J. Savage, and M.B. Wise, Nucl. Phys. B **478** (1996) 629 [nucl-th/9605002].
 - [6] D.B. Kaplan, M.J. Savage, and M.B. Wise, Phys. Lett. B **424** (1998) 390 [nucl-th/9801034].
 - [7] D.B. Kaplan, M.J. Savage, and M.B. Wise, Nucl. Phys. B **534** (1998) 329 [nucl-th/9802075].
 - [8] U. van Kolck, Eur. Phys. J. A **56**, no.3, 97 (2020) [arXiv:2003.09974 [nucl-th]].
 - [9] H.-W. Hammer, S. König, and U. van Kolck, Rev. Mod. Phys. **92** (2020) 025004 [arXiv:1906.12122 [nucl-th]].
 - [10] A. Manohar and H. Georgi, Nucl. Phys. B **234** (1984) 189.
 - [11] H. Georgi, Phys. Lett. B **298** (1993) 187 [hep-ph/9207278].
 - [12] S. Fleming, T. Mehen, and I.W. Stewart, Nucl. Phys. A **677** (2000) 313 [nucl-th/9911001].
 - [13] S. Fleming, T. Mehen and I. W. Stewart, Phys. Rev. C **61**, 044005 (2000) [arXiv:nucl-th/9906056 [nucl-th]].
 - [14] D.B. Kaplan and J.V. Steele, Phys. Rev. C **60** (1999) 064002 [nucl-th/9905027].
 - [15] D.B. Kaplan, Nucl. Phys. B **494** (1997) 471 [nucl-th/9610052].
 - [16] P. F. Bedaque and H. W. Griesshammer, Nucl. Phys. A **671**, 357-379 (2000) [arXiv:nucl-th/9907077 [nucl-th]].
 - [17] J. Soto and J. Tarrus, Phys. Rev. C **78**, 024003 (2008) [arXiv:0712.3404 [nucl-th]].
 - [18] J. Soto and J. Tarrus, Phys. Rev. C **81**, 014005 (2010) [arXiv:0906.1194 [nucl-th]].
 - [19] B. Long, Phys. Rev. C **88**, no.1, 014002 (2013) [arXiv:1304.7382 [nucl-th]].
 - [20] M. Sánchez Sánchez, C.-J. Yang, B. Long, and U. van Kolck, Phys. Rev. C **97** (2018) 024001 [arXiv:1704.08524 [nucl-th]].
 - [21] J. B. Habashi, M. Sánchez Sánchez, S. Fleming and U. van Kolck, in preparation.
 - [22] P. F. Bedaque, H. W. Hammer and U. van Kolck, Phys. Lett. B **569**, 159-167 (2003) [arXiv:nucl-th/0304007 [nucl-th]].
 - [23] S. Weinberg, Phys. Rev. **130**, 776-783 (1963)

- [24] S. Weinberg, Phys. Rev. **131** (1963) 440.
- [25] R. Peng, S. Lyu and B. Long, Commun. Theor. Phys. **72**, no.9, 095301 (2020)
- [26] <http://nn-online.org>.
- [27] V. G. J. Stoks, R. A. M. Klomp, M. C. M. Rentmeester and J. J. de Swart, Phys. Rev. C **48**, 792-815 (1993)
- [28] M.E. Luke and A.V. Manohar, Phys. Lett. B **286** (1992) 348.
- [29] E.E. Jenkins and A.V. Manohar, Phys. Lett. B **255** (1991) 558.
- [30] S. Weinberg, Phys. Rev. **166**, 1568-1577 (1968)
- [31] N. , R. Brockmann and W. Weise, Nucl. Phys. A **625**, 758-788 (1997) [arXiv:nucl-th/9706045 [nucl-th]].
- [32] J.R Taylor, *Scattering Theory: The Quantum Theory of Nonrelativistic Collisions*, Wiley, New York (1972).
- [33] D. R. Phillips, S. R. Beane and M. C. Birse, J. Phys. A **32**, 3397-3407 (1999) [arXiv:hep-th/9810049 [hep-th]].
- [34] G. Rupak and N. Shores, Phys. Rev. C **60**, 054004 (1999) [arXiv:nucl-th/9902077 [nucl-th]].
- [35] M. Pavón Valderrama, M. Sánchez Sánchez, C. J. Yang, B. Long, J. Carbonell and U. van Kolck, Phys. Rev. C **95**, no.5, 054001 (2017) [arXiv:1611.10175 [nucl-th]].
- [36] A. Nogga, R. G. E. Timmermans and U. van Kolck, Phys. Rev. C **72**, 054006 (2005) [arXiv:nucl-th/0506005 [nucl-th]].
- [37] B. Long and C. J. Yang, Phys. Rev. C **84**, 057001 (2011) [arXiv:1108.0985 [nucl-th]].
- [38] B. Long and C. J. Yang, Phys. Rev. C **85**, 034002 (2012) [arXiv:1111.3993 [nucl-th]].
- [39] S. Wu and B. Long, Phys. Rev. C **99**, no.2, 024003 (2019) [arXiv:1807.04407 [nucl-th]].
- [40] D. B. Kaplan, Phys. Rev. C **102**, no.3, 034004 (2020) [arXiv:1905.07485 [nucl-th]].
- [41] T. Mehen and I. W. Stewart, Phys. Lett. B **445**, 378-386 (1999) [arXiv:nucl-th/9809071 [nucl-th]].